

Tunable and Reconfigurable Terahertz Devices Based On Photo-Induced Electromagnetic Band Gap Structures

Jun Ren^{1*}, Yijing Deng¹, Zhenguo Jiang¹, Md. Itrat Bin Shams¹, Patrick Fay¹, and Lei Liu¹

¹University of Notre Dame, Notre Dame, 46556, USA

*Contact: jren1@nd.edu

Abstract—In this paper, we report the design and simulation of two optically controlled tunable and reconfigurable G-band (140-220 GHz) waveguide devices based on electromagnetic band gap (EBG) structures. The first device based on a pre-patterned EBG structure can be reconfigured between a band-stop filter (BSF) and a transmission line. The second device based on photo-induced EBG structures using a mesa-array shows increased level of tunability and reconfigurability with a BSF center frequency tunable from 175-200 GHz. The proposed tunable and reconfigurable THz devices are promising for a wide range of applications including multiple-frequency-band THz wireless communications.

I. INTRODUCTION

The realization of tunable and reconfigurable terahertz (THz) devices is essential to the implementation of advanced THz imaging and adaptive THz wireless communication systems, but is challenging using conventional approaches such as employing metamaterials, liquid-crystal-based devices, graphene modulator arrays, thermal sensitive elements, etc. [1, 2]. Although electromagnetic band gap (EBG) structures have been regarded as one promising solution for achieving dynamical control of broadband electromagnetic waves for a wide range of applications, existing EBG-based devices suffer from several key drawbacks including the requirement of complex fabrication processes [3] and limited tunability/reconfigurability [4], and therefore their usage as building blocks for high-performance tunable and reconfigurable THz devices is limited at present.

Recently, our group proposed and developed a novel optical control methodology for realizing tunable and reconfigurable THz devices [5-8]. The photogenerated free carriers in semiconductors were used to spatially modulate incident THz waves for implementing various functionalities. A number of demonstrations, including reconfigurable coded-aperture imaging masks [5], dynamically beam steering and forming antennas [6], and optically controlled variable waveguide attenuators/modulators [7, 8], have been reported. Besides, such an optical tuning methodology has been applied into the design of photo-induced EBG component at microwave frequencies [9]. An optically controlled tunable and reconfigurable microwave frequency filter based on the photo-induced EBG components has been studied and demonstrated,

whose functionality can be reconfigured between a band-stop filter (BSF) and a transmission line, and its center frequency can be tuned from 8-12 GHz by changing period of the virtual patterns illuminated onto the device [9].

In this paper, we further extend our previous work and apply the optical control methodology into the design of photo-induced EBG components for operation at THz frequencies. We will present two optically controlled G-band (140-220 GHz) waveguide components based on EBG structures for implementing tunable and reconfigurable THz filters. The first design features a pre-patterned EBG ground, and its functionality can be reconfigured between a filter with a center frequency at around 180 GHz and a transmission line by changing the illumination condition of the device. The second design employs a photo-induced EBG ground implemented on a Ge mesa-array structure for achieving a higher level of tunability and reconfigurability. Simulations show that the center frequency of the filter can be tuned from 175-200 GHz by projecting virtual EBG patterns with different periods onto the Ge mesa-array structure. The demonstrated tunable and reconfigurable THz devices are promising for applications in a range of THz systems including high-speed adaptive wireless THz communication systems.

II. RECONFIGURABLE G-BAND WAVEGUIDE FILTER BASED ON PRE-PATTERNED EBG

A. Design

Figure 1 shows the structure of the optically controlled reconfigurable G-band waveguide filter based on pre-patterned EBG. It was implemented in a back-to-back waveguide configuration, and consists of two offset input and output G-band waveguide channels connected by an E-plane microstrip chip. The microstrip chip is placed in the microstrip channel, whose dimension has been optimized to achieve single mode propagation over the full waveguide frequency band. The microstrip chip consists of a 5- μ m-thick Ge thin film on the backside of a 120- μ m-thick quartz substrate. A \sim 6 mm long section of transmission line with waveguide probes at both ends was patterned on the topside of the quartz. The waveguide probes adopted a rectangular microstrip design,

similar to the one presented in [10]. A uniplanar EBG ground plane with a one-dimensional circular hole array was patterned on the backside of the Ge. The period of the hole array and the diameter of each hole are $620\ \mu\text{m}$ and $100\ \mu\text{m}$, respectively, to generate a distinctive stop-band response at around 180 GHz. For both the top conductor and the ground plane, the thickness of the gold is $2\ \mu\text{m}$. An opening was designed at the bottom of the waveguide block so that the backside of the microstrip chip can be illuminated for realizing tunability and reconfigurability. In experiment, 808-nm infrared laser diodes are employed for illumination.

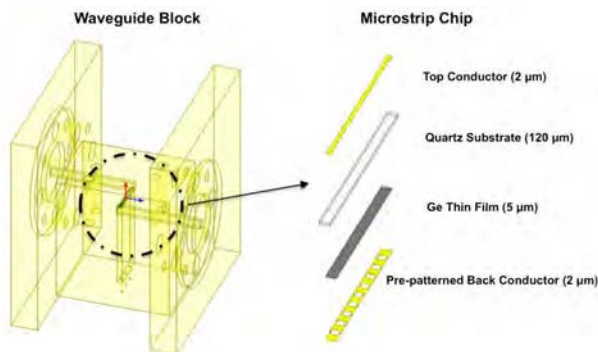


Fig. 1. Schematic drawing of the optically controlled reconfigurable G-band waveguide filter based on pre-patterned EBG. Detailed structure of the microstrip chip is shown.

B. Simulation

Full-wave HFSS simulation has been performed on the proposed waveguide filter above in the frequency range from 140-220 GHz. With no illumination, the simulation shows that the device exhibits a band-stop filter (BSF) behavior with a center frequency at around 180 GHz (see Fig. 2 (a)) as expected. The insertion loss in the pass-band is below 2 dB, and the stop-band rejection is larger than 12 dB. Fig. 2 (b) shows the simulated device response when the backside of the microstrip chip is illuminated with a light intensity of $34\ \text{W}/\text{cm}^2$. On the basis of the physics-based model we developed [11], such a level of incident light intensity results in a spatially averaged photoconductivity of $3 \times 10^5\ \text{S}/\text{m}$ in the illuminated Ge thin film with $5\ \mu\text{m}$ thickness (assuming a conservative value of $40\ \mu\text{s}$ for the effective carrier lifetime [8]). As a result, the BSF response disappears, and the device shows a transmission line response with an average of 1.5 dB insertion loss and better than 15 dB return loss over the full waveguide frequency band. Such a level of light intensity can be easily provided in experiment by illuminating the $\sim 6\ \text{mm}$ long EBG pattern area using our high power infrared laser diodes. These results indicate that the proposed G-band waveguide filter with pre-patterned EBG structure can be used to implement reconfigurable functionalities with high performance.

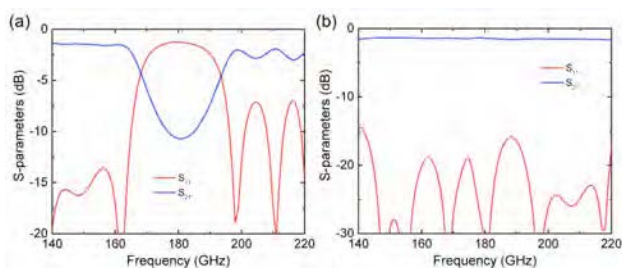


Fig. 2. Simulated frequency response of the optically controlled reconfigurable G-band waveguide filter based on pre-patterned EBG (a) without illumination, and (b) under $34\ \text{W}/\text{cm}^2$ illumination.

III. TUNABLE AND RECONFIGURABLE G-BAND WAVEGUIDE FILTER BASED ON PHOTO-INDUCED EBG

A. Design

Although the functionality of the waveguide device described in Section II can be reconfigured between a BSF and a transmission line, no tunability can be realized due to the employment of the pre-patterned gold layer. In order to demonstrate the full potential of the proposed optical control methodology in implementing tunable and reconfigurable THz devices, another G-band waveguide component based on photo-induced EBG structures was designed and simulated. Figure 3 illustrates the waveguide structure of the component. As shown in Fig. 3 (a), the component is implemented in the same back-to-back waveguide block as the first component described in Section II. Different from the first design, a $5\text{-}\mu\text{m}$ -thick Ge thin film without any pre-patterned gold layer was employed as the ground plane of the microstrip chip. By projecting required photo-patterns onto the Ge ground plane using a DMD chip unit in conjunction with laser diodes, EBG structures were virtually generated. For achieving circuit operation at THz frequencies, the required feature size is even smaller than the diffusion length of the Ge ($\sim 0.5\ \text{mm}$), which prevents reliable transfer of the photo-patterns from the DMD chip unit to the Ge. To overcome the limitation of achievable spatial resolution, a mesa-array structure was created on the Ge thin film. Detailed study on the mesa-array structures has been reported previously [9][11]. In this work, a simplified version of the mesa-array structure with trenches only cut along the transverse direction was employed. The trench size and mesa size were designed to be $0.1\ \mu\text{m}$ and $25\ \mu\text{m}$, respectively, to ensure that the mesa-array structure will not degrade the circuit performance while providing sufficiently high resolution. Rectangular (rather than circular) EBG patterns were projected onto the Ge mesa-array to create photo-induced EBG structures. The dimension of the photo-patterns was chosen to be integer multiples of the mesa size so that optical alignment can be easily achieved in experiment.

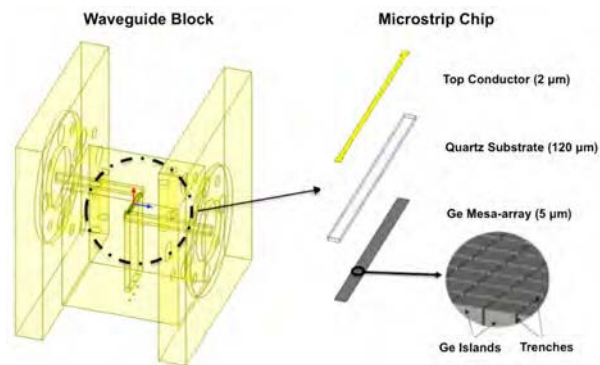


Fig. 3. Schematic drawing of the optically controlled reconfigurable G-band waveguide filter based on photo-induced EBG. Detailed structure of the microstrip chip with a mesa-array is shown.

B. Simulation

Figure 4 (a) shows the simulated S-parameters of the device from 140-220 GHz when a 34 W/cm^2 incident light is uniformly illuminating the mesa-array structure (as shown in Fig. 4 (b)). A spatially averaged photoconductivity of $3 \times 10^5 \text{ S/m}$ was used in the simulation for the illuminated Ge mesa-array with $5 \mu\text{m}$ thickness. It is seen that the device shows a transmission line response with $\sim 2 \text{ dB}$ insertion loss and better than 10 dB return loss over the full waveguide frequency band.

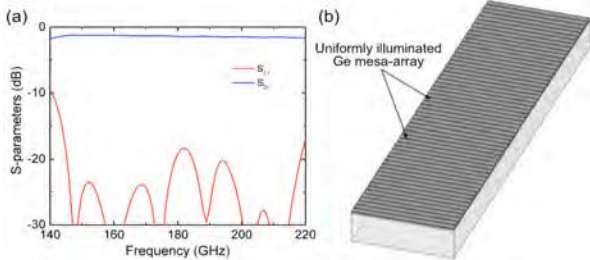


Fig. 4. (a) Simulated frequency response of the optically controlled reconfigurable G-band waveguide device (b) when the mesa-array structure is illuminated with 34 W/cm^2 uniform light.

When the mesa-array structure is illuminated with virtual EBG patterns, the device will be reconfigured to BSFs. This is demonstrated in Fig. 5. It is seen that when a virtual EBG pattern with a period of $625 \mu\text{m}$ and an un-illuminated area length of $275 \mu\text{m}$ is imposed onto the mesa-array, a BSF response with a center frequency at 175 GHz was shown. Since the center frequency of the BSF is inversely related to the period of the EBG pattern, it can also be tuned by imposing virtual EBG patterns with different periods. When the period of the photo-induced EBG patterns was varied from $625 \mu\text{m}$ to $525 \mu\text{m}$, and the length of the un-illuminated pattern was changed from $275 \mu\text{m}$ to $250 \mu\text{m}$, another BSF response with a center frequency at 200 GHz was observed. The stop-band rejection exceeds 10 dB in both cases, and the return loss in the stop-band is less than 3 dB . These results indicate that the waveguide component can not only achieve reconfigurable performance between a BSF and a transmission line, but also realize broadband tuning of the BSF center frequency in the THz domain with the much-improved spatial resolution enabled by the mesa-array structure. In addition, it should be noted that by employing a mesa-array with even smaller mesa size, even higher spatial resolution can be achieved, enabling continuous tuning of the center frequency.

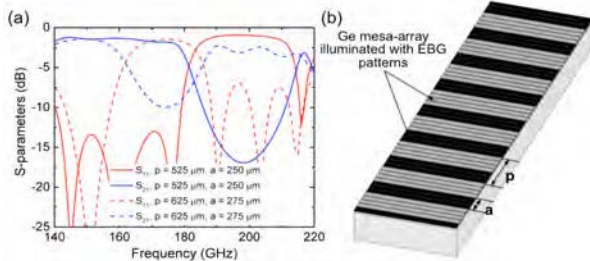


Fig. 5. (a) Simulated frequency response of the optically controlled reconfigurable G-band waveguide filter based on photo-induced EBG in response to (b) EBG patterns with various periods.

On the basis of the above study, it has shown that the proposed optically controlled waveguide component based on

photo-induced EBG can achieve high tunability and reconfigurability, and is promising for the implementation of high-performance dynamically tunable and reconfigurable filters operating at THz frequencies.

CONCLUSIONS

Two optically controlled tunable and reconfigurable G-band waveguide devices based on EBG structures have been designed and simulated. The first device based on a pre-patterned EBG structure shows reconfigurable performance between a BSF and a transmission line. The second device based on photo-induced EBG structures presents increased level of tunability and reconfigurability by employing a mesa-array structured ground. A broad tuning range of BSF center frequency from $175\text{-}200 \text{ GHz}$ has been demonstrated in simulations. The proposed tunable and reconfigurable THz devices based on photo-induced EBG are promising for a wide range of applications including multiple-frequency-band THz wireless communications.

ACKNOWLEDGMENT

This work is partially supported by the National Science Foundation (NSF) under the grant of ECCS-1711631 and ECCS-1711052, and a subcontract from the Harvard-Smithsonian Center for Astrophysics under grant PTX-Smithsonian 17-SUBC-400SV787007. The authors would like to thank the support from Center for Nano Science and Technology (NDnano) and Advanced Diagnostics & Therapeutics (AD&T) at the University of Notre Dame.

REFERENCES

- [1] M. Tonouchi, "Cutting-edge terahertz technology", *Nature photonics*, 1(2), pp. 97-105, 2007.
- [2] K. C. Huang, and Z. Wang, "Terahertz terabit wireless communication", *IEEE Microwave Magazine*, 12(4), pp. 108-116, 2011.
- [3] A. Delustrac, F. Gadot, E. Akmansoy, and T. Brillat, "High-directivity planar antenna using controllable photonic bandgap material at microwave frequencies," *APhys. Lett.*, Vol. 78, 4196, 2002.
- [4] L. Mercier, M. Thevenot, P. Blonby, and B. Jecko, "Design and characterization of a smart periodic material including MEMS," *Proc. 27th ESA Antenna Technology Workshop on Innovative Periodic Antennas: Electromagnetic Bandgap, Left-Handed Materials, Fractal and Frequency Selective Surfaces*, Santiago de Compostela, Spain, March 2004.
- [5] M. I. B. Shams, Z. Jiang, S. Rahman, J. Qayyum, L.-J. Cheng, H. G. Xing, P. Fay, L. Liu, "Approaching real-time terahertz imaging with photo-induced coded apertures and compressed sensing," *IET Electron. Lett.*, vol. 50, no. 11, pp. 801-803, 2014.
- [6] M. I. B. Shams, Z. Jiang, J. Qayyum, S. Rahman, P. Fay, and L. Liu, "A Terahertz reconfigurable photo-induced fresnel-zone-plate antenna for dynamic two-dimensional beam steering and forming," *International Microwave Symposium*, 1-4, Phoenix, Arizona, 2015.
- [7] Z. Jiang et al., "Investigation and demonstration of a WR-4.3 optically controlled waveguide attenuator," *IEEE Trans. THz Sci. & Tech.*, vol. 7, no. 1, pp. 20-26, 2017.
- [8] J. Ren et al., "High-performance WR-4.3 optically controlled variable attenuator with 60-dB range," *IEEE Microw. Wire. Comp. Lett.*, vol. 28, no. 6, pp. 512-514, 2018.
- [9] J. Ren et al., "Photo-induced electromagnetic band gap structures for optically tunable microwave filters", *Progress in Electromagnetics Research*, vol. 161, no. 1, pp. 101-111, 2018.
- [10] J. L. Hesler, W. R. Hall, T. W. Crowe, R. M. Weikle, B. S. Deaver, R. F. Bradley, Djerafi, and S. K. Pan, "Fixed-tuned submillimeter wavelength

waveguide mixers using planar schottky-barrier diodes”, IEEE MTT, vol. 45, pp. 653–658, 1997.

- [11] A. Kannegulla, M. I. B. Shams, L. Liu, and L. -J. Cheng, “Photo-induced spatial modulation of THz waves: Opportunities and limitations,” *Opt. Exp.*, vol. 23, no. 25, pp. 32098– 32112, 2015.